



Groundwater Vulnerability Assessment Using Different Overlay and Index Methods for Quaternary Aquifer of Wadi El-Tumilat, East Delta, Egypt

GAD, M. I.^{1*} --- El-Kammar, M. M.² --- Ismail, H. M. G.³

^{1,3}Hydrology Division, Desert Research Center, El-Mataryah, Cairo, Egypt

²Geology Department, Faculty of Science, Cairo University, Cairo, Egypt

Abstract

Contamination from rapid urban development, industrialization and agricultural sources increasingly threatens the groundwater resource in the shallow phreatic Quaternary Aquifer of the Wadi El-Tumilat (QAWT), East Delta, Egypt. In this paper, fourteen environmental sensitive heavy metals and two minor elements (PO_4^- and NO_3^-) were checked by the chemical analysis of both 25 surface and groundwater samples at 2006. An assessment of the QAWT intrinsic vulnerability was carried out in this paper based on GOD, PRAST and DRASTIC methods. The calculated vulnerability indexes resulted from the three methods showed great differences due to the different criterions used. Moreover, a weight modification was assumed to adequate the arid zone. The obtained QAWT vulnerability maps showed the high extension of medium vulnerability zones. The high vulnerability zones occupied about 35% and 31% from applying PRAST and DRASTIC methods respectively. The high vulnerability in these areas was mainly related to the low values of depth to water (less than 10 m), the high permeability of the soils (9 m/day) and the high permeability of the vadose zone materials (more than 11 m/day). The most suitable areas for new reclamation activity were located in the southern boundary of Wadi El Tumilat especially the strip south El Mahsama drain by 5 km. These resulted maps may provide planners with tools for a preliminary selection of priority areas for different forms of sustainable development.

Keywords: Hydrogeology, Vulnerability assessment, Wadi El-Tumilat, GOD, PRAST, DRASTIC methods.



This work is licensed under a [Creative Commons Attribution 3.0 License](https://creativecommons.org/licenses/by/3.0/)
Asian Online Journal Publishing Group

Contents

| | |
|---|----|
| 1. Introduction..... | 10 |
| 2. Materials and Methods | 12 |
| 3. Results and Discussion | 16 |
| 4. Conclusion and Recommendations | 21 |
| References..... | 21 |

1. Introduction

The term “vulnerability of groundwater to contamination” was first used by Margat [1]. Vowinkel, et al. [2] defined vulnerability as sensitivity plus intensity, where intensity is a measure of the source of contamination. Intrinsic vulnerability is controlled exclusively by geological structure and hydrogeological conditions, while specific vulnerability includes, besides the former parameters, consideration of the type of a contaminant and the character of a contamination source [3].

In this paper, due to the groundwater contamination in some plots of the Quaternary Aquifer of Wadi El Tumilat (QAWT), a trial to assess the intrinsic groundwater vulnerability was carried out applying three different methods to delineate the less vulnerable areas suitable for new reclamation activities.

1.1. Location of the Studied Area

The QAWT lies between latitudes $30^{\circ}25'$ and $30^{\circ}35'$ N and longitude $31^{\circ}45'$ and $32^{\circ}20'$ E. It is bounded on the NW by Bahr El Baqar Drain, on the west by Wadi El Watan, on the east by Suez Canal and its attached lakes and on the south by Cairo-Shubrawit Ridges with total area of magnitude 1500 km^2 (Figu5r4e 1). It is characterized by desert climate, with arid, hot and rainless summer, and mild winter with low precipitation (22-40 mm/year). The evaporation rate is very high (6-12 mm/day).

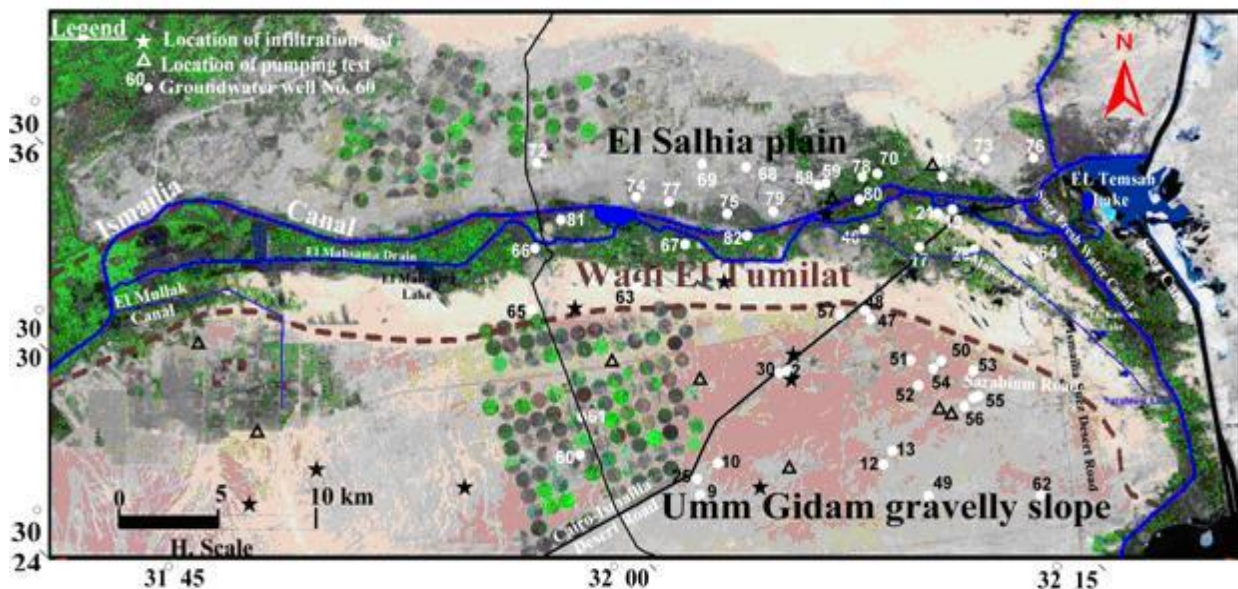


Figure-1. Location map of the infiltration tests, pumping tests and monitored wells in the QAWT

1.2. Geomorphological Aspects

In the literatures [4-7], Wadi El Tumilat represents a part of the eastern gravelly slopes fringing the Nile Delta and bears the structural affinity to the Syrian arc system. The northern limit is defined by the well known buried Nile branch "Pelusaic" which extends in NE-SW direction and is represented by a semi flat plain called El Salhia plain (Figure 2). El Timsah and Bitter lakes represent the remnants of an old structural and topographic low land area called Isthmus Stretch along the eastern boundaries. The southern boundary of Wadi El-Tumilat is represented by Umm Gidam gravelly sand sheets in the form of low lying slopes. The southern boundary is determined by a series of structural ridges extend in an E-W trend. The foreland slopes of the southern structural ridges are dissected by few morphotectonic main drainage lines, mostly of NW-SE trend with numerous dendritic tributaries (Figure 2).

1.3. Geological Aspects

The study area is built up of sedimentary rocks belonging to both Tertiary and Quaternary ages (Figure 2) with thickness more than 1500 m (Table 1) [5, 7-13]. Tertiary rocks are exposed south of the study area and represented by Eocene, Oligocene, Miocene and Pliocene units (Figure 2). Middle and Upper Eocene rocks are formed of shallow marine fossiliferous chalky, dolomitic sandy and marly limestones. Oligocene rocks are exposed in the area between Cairo and Suez at Gebel Umm El Ragm and Gebel Umm Qamar. They are formed of continental sands and gravels as well as volcanic basalts with variable thickness ranging from 45 m at Gebel Iwiebid to 100 m at Gebel El Nassuri area. Miocene rocks are composed of sandy limestone and sandy marls of shallow marine origin and are represented by El Shatt Formation and El Hommath Formation. Pliocene rocks are exposed in the area northwest of Cairo along the margins of the Heliopolis basin. Quaternary deposits have a wide distribution represented by old deltaic deposits which are composed of fluvial coarse quartz sand, cherty flinty pebbles and igneous fragments with few occasional fossil wood remains and young Aeolian deposits. The subsurface sedimentary succession is also built of Tertiary and Quaternary rocks, Tertiary rocks include Miocene sandy limestone water bearing Formation and Pliocene impermeable shale and clay beds. The regional structure of the study area is homoclinal having a low northward dip. This dip controls the thickness of some aquifers. It forms the foreland side of the ancient Mediterranean geosyncline. Normal faults are the most conspicuous structural elements affecting the landscape in this area, and are dominantly represented by NE-SW trend with downthrown side toward SE and NW and NW-SE trend with downthrown side toward NE direction. The vertical displacement along these faults ranges from few meters to hundred meters which led to an increase of the thickness of the Quaternary water bearing Formation by due 3 m/km towards northeast direction [13].

1.4. Hydrogeological Conditions

The water bearing formations in the Wadi El-Tumilat area comprise the QAWT, occupies the shallow zone and the Miocene aquifer dominating the deeper part [14]. The QAWT represents the main aquifer in the region and composed of fluvial and fluvio-marine graded sand and gravel with clay intercalations of limited extension (Figure 3). The basal portion of this aquifer is formed of dark plastic clay. The Quaternary deposits rest directly with unconformity surface on the Miocene hard limestone as recognized in the north and south of Wadi El-Tumilat. Its total thickness increases generally from south to north. It is mainly recharged by Nile water from the river branches and canals. The Miocene aquifer is dominated by clastic facies in the southern part of the study area and overlain by about 200 m of Quaternary deposits [15]. In Belbies-El Tell El Kabier-El Salhiya fluvial plain, the Miocene sediments are composed of alternating sandy limestone and clay lenses, loose quartz sand and marl. The aquifer is more clayey towards east. The cross-section along the QAWT monitoring well line (Figure 3) shows the general characteristics of the mode of groundwater occurrences. It is clear that, the clay intercalations are generally existed towards south and north. In the narrow strip adjacent to the Ismailia canal, the depth to the groundwater is highly affected by the surface water running in the canal.

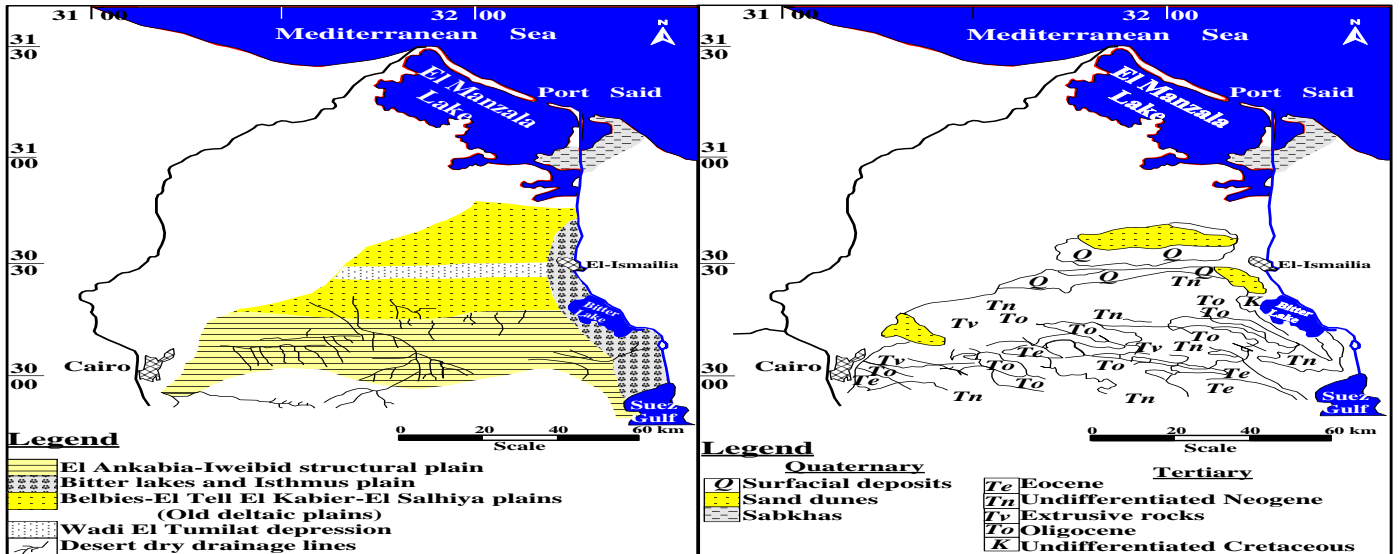


Figure-2. Geomorphologic map (left map) and the compiled geological map after geological map of Egypt, 1971 (right map) of the East Delta

Table-1. Sedimentary succession in the study area

| Age | Lithology | Approximate Thickness (m) |
|-------------|--|---------------------------|
| Eocene | Chalky limestone, sand and clay | 432 |
| Oligocene | Sand, gravel and basalt | 264 |
| Miocene | Sandy limestone and clay | 224 |
| Pliocene | Marine clay | 192 |
| Pleistocene | Fine sand and gravelly calcareous sand | 352 |
| Recent | Aeolian sand and silt | 40 |

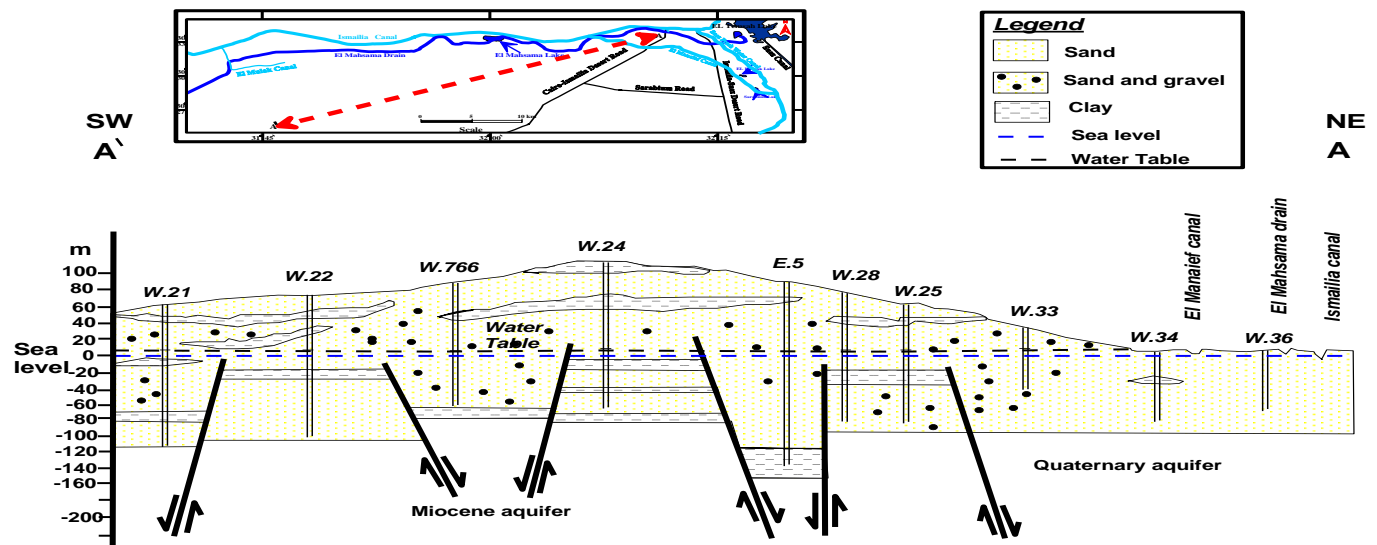


Figure-3. The cross-section along the QAWT monitoring well line in NE-SW direction showing different water bearing formations (after Gad [13])

The QAWT and the Miocene aquifers are hydraulically connected but in some places, they are separated by a semi-permeable layer which is highly controlled by deep-seated faults. These faults cause the saline groundwater of Miocene aquifer to move upward along the fault planes and mixed with the groundwater of the QAWT [13]. The groundwater in the QAWT ranges from unconfined in the western part to semi-confined in the eastern part due to the presence of capped and underlying clay beds.

The groundwater flow in the QAWT is directed mainly from south to north in the southern part (Miocene aquifer) with very low hydraulic gradient ($\approx 2 \times 10^{-4}$). An opposite direction is recorded from north to south in the area lying south of Ismailia canal (hydraulic gradient $\approx 4 \times 10^{-4}$). Along the main flood plain and down stream of Wadi El

Tumilat, an opposite direction is recorded from north to south (local flow) in the area lying south of Ismailia canal (the hydraulic gradient is about 8×10^{-4}). The main groundwater recharging source is the Ismailia canal while Suez and El-Manaief fresh water canals are additional sources. In the Western and eastern parts of the QAWT, a general trend of discharge in W-E direction is observed due to the intensive pumping of groundwater for reclamation projects at Wadi El-Mullak, El-Manaief and Sarabium occupying the central part (Figure 4, Ismail [16]).

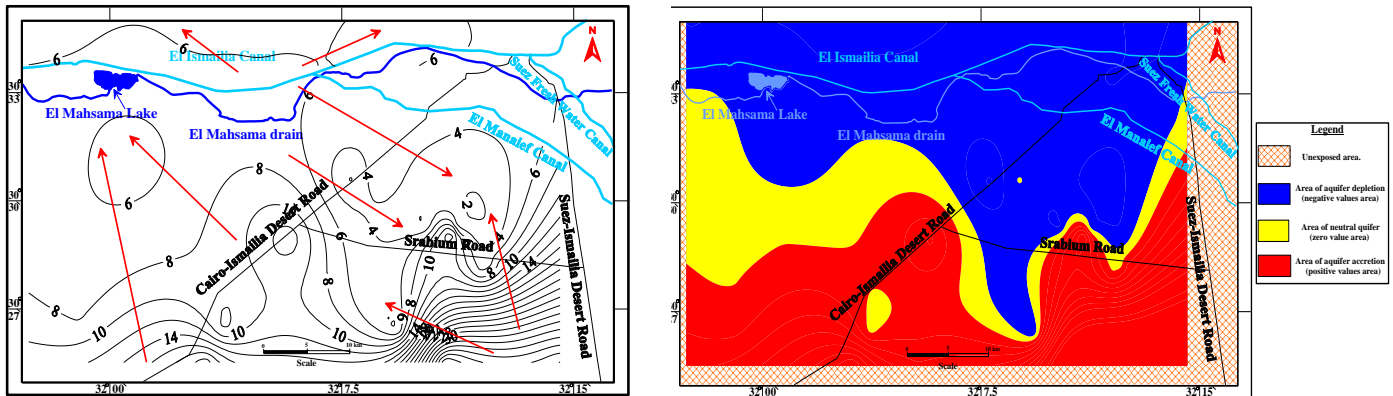


Figure-4. Water table map at Dec. 2005 (left map) and water table fluctuation map during 1992-2005 (right map, Ismail [16]) of the QAWT

The constructed water table fluctuation map over the period Dec. 1992- Dec. 2005 reflects the wide change in the water table values during this interval (Figure 4). This reflects the need for intrinsic rather than specific vulnerability assessment. On the contrary, the uncultivated flat areas in the central flood plain of the QAWT reveal no changes in the groundwater storage. The most deteriorated areas are those lying in the northern lowlands of the QAWT while the least deteriorated areas are located in the southeastern part of it. The main irrigation canals network (Suez fresh water canal and El Manaief canal), the main drainage network (El Mahsama drain, El Mahsamalake, El Karnak lake, El Manaief lake and Sarabium lake) play a significant role in the groundwater pollution in the QAWT based on its vulnerability.

2. Materials and Methods

The materials used in this paper are collected through carrying out four field trips in QAWT area during the period 2005-08 with the team work of the Desert Research Center. These materials include collection of archival well data (discharge, distribution, operating systems,...etc.) beside carrying out both pumping and infiltration tests representing the different soils in the QAWT. The four infiltration test are performed using the double ring method, as described by Black [17] and the field data are analyzed according to Philip [18] beside archival data of six tests carried out by Gad [13] and two tests by Afify [19]. Complete chemical analyses of both 26 surface water and 28 selected groundwater samples are performed in the Central Lab of the Desert Research Center during the year 2005-07 according to the methods adopted by the U.S Geological Survey, Rainwater and Thatcher [20]. In addition, the environmental sensitive heavy metals and minor elements including Al, B, Cd, Co, Cr, Cu, Fe, Mn, Mo, Ni, Pb, Sr, V, Zn, PO₄ and NO₃ are evaluated to clarify the industrial and agricultural pollution. Moreover, the following maps are prepared:

2.1. Depth to Water Map

Depth to water parameter represents the depth of the water table from the topographic surface and gives an idea of the minimum distance that a pollutant has to travel to reach the saturated zone. Depth to water was computed based on the field data during 2005. The recorded depth to water in the selected wells was used in constructing the depth to water map.

2.2. Net Recharge Map

The weighted net recharge depends mainly on the constructed isohyetal map of the QAWT based on the meteorological data of the period 1936-993. The computed net recharge values in the selected points are equal to the difference between precipitation plus return flow after irrigation minus the evapotranspiration. Applying the number of points for each value (Table 2), the weighted net recharge map is constructed.

Table-2. Assessment of net recharge [21]

| Net recharge (mm/year) | No. of points |
|------------------------|---------------|
| 0 – 50 | 1 |
| 50 – 100 | 3 |
| 100 – 180 | 6 |
| 180 – 250 | 8 |
| >250 | 9 |

2.3. Aquifer Media Map

Aquifer media information is depicted from the three major maps (the diffusivity, lithology cover and aquifer thickness maps). The diffusivity values were resulted from dividing the transmissivity T and the storativity S (or specific yield Sy in case of unconfined aquifer). The Transmissivity T and the storativity S is estimated from the

carried out five pumping tests and four recovery tests in addition to other eight tests from previous work. Theis [22] type curve method, Cooper and Jacob [23] straight line method and Theis recovery method are used in the analysis of these data. The weighted diffusivity map has been prepared by multiplying the diffusivity value (T/S) for every borehole by its aquifer saturated thickness and the output data were organized in GIS format through which the successive weighed diffusivity at each well can be determined. Repeating the same steps for the other two parameters, the weighted aquifer media map is obtained.

2.4. Soil Media Map

The soil media map is very important because it determines the overall protective effectiveness of the soil and rock covers above the shallow aquifers. It reflects the main properties of the soil zone as effective field capacity (eFC), cation exchange capacity (CEC) and electric conductivity of the soil (EC). The eFC, CEC and EC analyses resulted from the deep soil profile of the QAWT sited in Shata [24] (Table 3) is used in developing the soil media map.

Table-3. The available data of soil parameters of the different soil profiles in the study area (after Shata [24])

| Soil profile N. | Soil depth (m) | eFC | CEC | EC | Soil texture |
|-----------------|----------------|-----|-------|------|--------------|
| 1 | 0 – 0.2 | 8 | 6.36 | 820 | Sand |
| | 0.2 – 0.5 | 22 | 43.46 | 95 | Loam |
| | 0.5 – 1 | 22 | 56.51 | 32 | Loam |
| 2 | 0 – 0.1 | 8 | 1.34 | 1.5 | Sand |
| | 0.1 – 0.35 | 8 | 6.85 | 4.5 | Sand |
| | 0.35 – 0.7 | 8 | 6.47 | 6 | Sand |
| | 0.7 – 1.5 | 8 | 1.63 | 5.5 | Sand |
| 3 | 0 – 0.25 | 8 | 3.69 | 2.5 | Sand |
| | 0.25 – 0.35 | 8 | 4.29 | 16 | Sand |
| | 0.35 – 1 | 8 | 6.36 | 24.5 | Sand |
| 4 | 0 – 0.15 | 8 | 7.66 | 7 | Loamy sand |
| | 0.15 – 0.45 | 8 | 4.89 | 8 | Sand |
| | 0.45 – 0.75 | 8 | 4.29 | 0.75 | Sand |
| | 0.75 – 2 | 8 | 3.69 | 0.45 | Sand |
| 5 | 0 – 0.15 | 8 | 5.11 | 11 | Sand |
| | 0.15 – 0.6 | 8 | 4.89 | 16.5 | Sand |
| | 0.6 – 0.75 | 8 | 7.28 | 17.5 | Sand |
| | 0.75 – 1.5 | 8 | 4.24 | 18 | Sand |
| 6 | 0 – 0.72 | 8 | 2.07 | 0.95 | Sand |
| | 0.72 – 1.05 | 8 | 2.17 | 0.8 | Sand |
| | 1.05 – 1.2 | 8 | 43.48 | 0.6 | Loamy sand |

eFC is effective field capacity, CEC is cation exchange capacity and EC is electric conductivity of the soil

2.5. Topography Map

It is represented by steepness percent. Areas with steep slopes are less vulnerable to groundwater contamination. The Digital Elevation Model map (90 m x 90 m DEM-map) obtained from Shuttle Radar Topography Mission (SRTM) is used in extracting the topographic feature of the QAWT. Accordingly, the DEM-map is modeled on GIS platform using GIS Software to define the slope of each cell.

2.6. Impact of Vadose Zone Map

The impact of vadose zone involves two main parameters of the unsaturated zone, the thickness of clay lenses and the soil infiltration rate. The clay content is an important parameter for adsorption processes, and to a slightly lesser extent for cation exchange and biodegradation processes. The weighted clay lenses' thickness is developed as described by Bodenkunde [25], (Table 4).

Table-4. Assessment of unconsolidated rocks (number of points = R_u), by Bodenkunde [25]

| Type of unconsolidated rock | R_u = No. of points per meter bed thickness |
|---|---|
| Clay | 500 |
| Loamy clay, slightly silty clay | 400 |
| Slightly sandy clay | 350 |
| Silty clay, clayey silty loam | 320 |
| Clayey loam | 300 |
| Very silty clay, sandy clay | 270 |
| Very loamy silt | 250 |
| Slightly clayey loam, clayey, silty loam | 240 |
| Very clayey silt, silt loam | 220 |
| Very sandy clay, sandy silty, loam, slightly sandy loam, loamy silt | 200 |
| Sandy loam, slightly loamy silt | 180 |
| Slightly loam, silt, sandy loamy silt, silt, slightly sandy loam. | 160 |

Continue

| | |
|---|-----|
| Very clayey sand, clayey sand, loamy silty sand | 140 |
| Sandy silty, very loamy sand | 120 |
| Loamy sand, very silty sand | 90 |
| Slightly clayey sand, silty sand, sandy clayey gravel | 75 |
| Slightly loamy sand, sandy silty gravel | 60 |
| Slightly silty sand, slightly silty sand with gravel | 50 |
| Sand | 25 |
| sand with gravel, sandy gravel | 10 |
| gravel, gravel and breccia | 5 |
| unconsolidated volcanic material | 200 |
| Peat | 400 |
| Sapropel | 300 |

In the other side, the methodological approach used in this paper is based on the vulnerability modeling techniques using a range of different methods [3, 21, 26-36]. Unfortunately, no unified methodology of vulnerability assessment has been accepted in the QAWT although the problem has been presented in several works [16, 37-40]. This may attribute to the complexity and variability of recharge and groundwater flow conditions in the hydrogeological medium. For this reason, when developing the current concept for the intrinsic groundwater vulnerability map of QAWT, the authors based it not only on the use of concepts published abroad but also on their own experience.

2.7. Intrinsic Vulnerability Methodology

Intrinsic vulnerability is assessed by the GOD, PRAST and DRASTIC overlay and index methods. The first GOD method [27, 41] considers the susceptibility of the aquifer to the entry of contaminants from the topographic surface. The following variables are analyzed: groundwater occurrence (G), overall lithology of aquifer or aquitard (O) and depth to groundwater table (D). The D factor depends on aquifer recharge. The marked irrigation system irregularity, both flooding and drip irrigation, that is typical in QAWT, requires defining a specific period when evaluating the vulnerability of the QAWT to contamination. Vulnerability should be analyzed for the situation of greatest risk of groundwater contamination, that is, one corresponding to a period of high levels of irrigation, favoring aquifer recharge and the transport of contaminant materials, Goldscheider and Popescu [42]. QAWT recharge from return flow after irrigation and seepage from the surface water bodies produce a rise in the piezometric level and thus increased vulnerability, due to the reduced transit time between the entry of potential sources of contamination and their contact with the groundwater. According to Vrba and Zaporozec [3] and Civita [43], the GOD method comprises a mapping overlay based on a factor-scoring system. The variables G, O and D are obtained from the field measurements and the different constructed maps. The super-position of these three information layers is performed within a Geographic Information System (GIS), which is used to calculate the index and classes of vulnerability where the GOD Index reads:

$$\text{GOD vulnerability index} = \text{Rating for Groundwater occurrence} \times \text{Rating for Overlaying lithology (only in case of unconfined aquifers)} \times \text{Rating for Depth to water} \dots\dots\dots 1$$

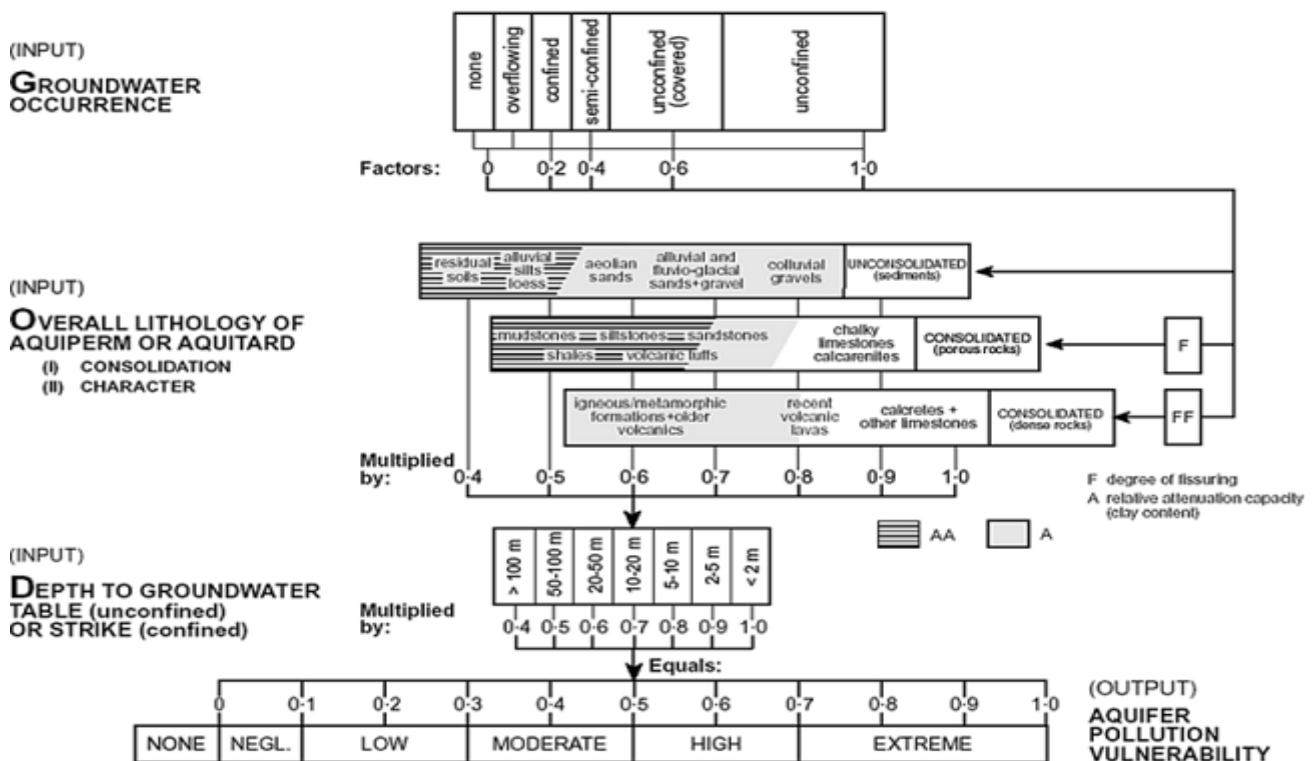


Figure-8. GOD overlay and index system of aquifer vulnerability assessment (after Foster and Hirata [41])

In addition, the second PRAST rating system [43] is another method for quick assessment of vulnerability using five parameters: Protective effectiveness, Net Recharge, Aquifer media, Soil media and Topography. The overall "Pollution Potential" or PRAST Index PI is established by applying the following formula:

$$PI = P_r \times P_w + R_r \times R_w + A_r \times A_w + S_r \times S_w + T_r \times T_w \dots \dots \dots 2$$

Where **r** is the rating value and **w** is the weight associated to each parameter. The ratings in PRAST model were assigned values between 1 and 10, while the weight of every factor had a fixed value which is listed in Table 5.

Table-5. Assigned weights for PRAST parameters.

| Parameter | Weight |
|--------------------------|--------|
| Protective effectiveness | 8 |
| Net Recharge | 4 |
| Aquifer Media | 3 |
| Soil Media | 2 |
| Topography | 1 |

One of the most widely used groundwater vulnerability methods is the third chosen method; i.e., DRASTIC [26] and developed by the United States Environmental Protection Agency (US EPA) [44] as a method for assessing groundwater pollution potential. In the DRASTIC method specific criteria are assigned different degrees of importance on a scale 1 to 5 (Table 6). These criteria including: depth to water level, effective infiltration, aquifer media, type of soil, topography, impact of vadose zone, and the hydraulic conductivity of aquifer. Vulnerability DRASTIC index DI is the sum of the multiplication of variable rank and weight of individual criterion. For each mapping unit, it is calculated using the most important seven different hydrogeological parameters that affect the potential for groundwater pollution. It is computed as [45-51]:

$$DI = D_r \times D_w + R_r \times R_w + A_r \times A_r + S_r \times S_w + T_r \times T_w + I_r \times I_w + C_r \times C_w \dots \dots \dots 3$$

Where D is the Depth to water, R is the net Recharge, A is the Aquifer media, S is the Soil media, T is the Topography, I is the Impact of the vadose zone, C is the hydraulic Conductivity, **r** is the rating value and **w** is the weight associated to each parameter. Each parameter is assigned the same weight all over the QAWT but different ratings, according to the hydrological, geological and hydrogeological conditions. The weight of three criterions (Soil media S, vadose zone media I and topography T) is modified to adapt the physical conditions of the QAWT. Worth mention, the soil media (S) and the impact of the vadose zone media (I) of the QAWT can be considered as one continuous layer of equal importance, and can thus be assigned an equal weight (5). Also, the DRASTIC criterion relative to the slope of topography is governed mainly by the prevailing irrigation practice in humid areas including mountainous, rugged and flat surfaces which is different in arid area like the QAWT with flat lands or lands with gentle slope. It modified from weight of 1 to 2.

Table-6. Rating and weight of criterion for DRASTIC criterions with assigned weights (after Aller, et al. [26]- modified for the QAWT)

| No | Criterion | Classes of criterion | Weight of criterion | Rank |
|----|----------------------------|---------------------------------|---------------------|----------|
| 1 | Depth to groundwater table | >5 m | 5 | 7 |
| | | 3.1- 5 m | | 8 |
| | | 1.1 – 3 m | | 9 |
| | | <1 m | | 10 |
| 2 | Net Recharge (mm/year) | 50-75 | 4 | 2 |
| | | 76-100 | | 3 |
| | | 101-125 | | 4 |
| | | 126-150 | | 5 |
| | | >150 | | 6 |
| | | | | |
| 3 | Lithology of Aquifer | Sandy clay, loam, loam and sand | 3 | 2 |
| | | Sandy loam, sands | | 3 |
| | | Sands, sandy loam | | 4 |
| | | Sands | | 6 |
| | | Sands, gravel | | 8 |
| 4 | Soil media | Loam | 5 | 5 |
| | | Sandy loam | | 6 |
| | | Shrinking clay | | 7 |
| | | Peat | | 8 |
| | | Thin anthropogenic | | 9 |
| | | Absent | | 10 |
| 5 | Topography (slope) (%) | 2.9-3.9 | 2 | 7.5 |
| | | 2.5-2.9 | | 8 |
| | | 2.0-2.5 | | 8.5 |
| | | 1.6-2.0 | | 9 |
| | | 1.0-1.6 | | 9.5 |
| | | 1.0-0.0 | | 10 |
| | | | | |
| 6 | Impact of vadose zone | Clay | 5 | 2 |
| | | Silty loam | | 3 |
| | | | | Continue |

| | | | | |
|---|---|---------------|---|---|
| 7 | Hydraulic Conductivity of aquifer (m/day) | Loam | 3 | 4 |
| | | Sands | | 6 |
| | | Sands, gravel | | 8 |
| | | < 9 | | 1 |
| | | 9-11 | | 2 |
| | | 12-28 | | 4 |
| | | 29-40 | | 6 |
| | | 41-80 | | 8 |

3. Results and Discussion

The results of the chemical analysis of the chosen groundwater samples of the QAWT show that the salinity distribution map (Figure 5) is well conformable with the water table map (Figure 4), where salinity increases gradually with the hydraulic gradient and vice versa. Also, the hypothetical salt assemblages change from north to south according to metasomatic processes. The effect of the evaporites in the eastern parts is more pronounced in the high salinity of their groundwater. Chloride water type is the dominant and exists by 86%, while the bicarbonate water type represents 14% only. The gradual increase of salinity and the change of water type in the QAWT reveal that, the groundwater has been subjected to physiochemical mixing processes during the beginning of the Holocene periods, cation exchange and the mixing of Nile water with locally infiltrated fossil water.

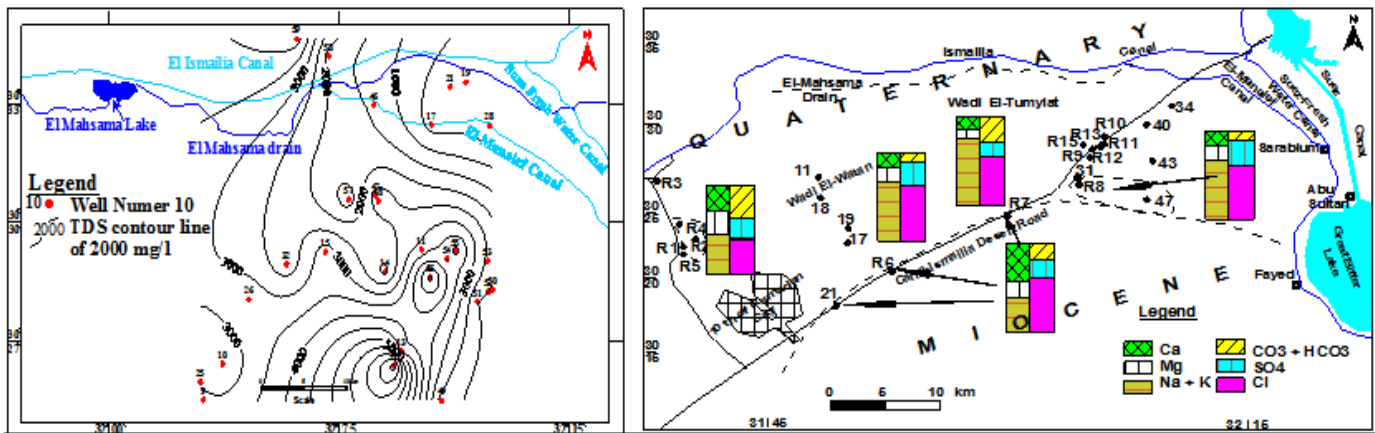


Figure-5. Salinity distribution map in mg/l (left) and the hypothetical salt assemblages (right map, Fatouh, et al. [52]) of the groundwater of the QAWT

The groundwater pollution is observed from the results of the chemical analysis of the 14 environmental sensitive heavy metals and two minor elements (Table 7). Both surface and groundwater are mostly polluted with B, Sr, V, PO₄⁻ and NO₃⁻ according to the World Health Organization Standards for Drinking Water (WHO) [53] and Egyptian Health Committee for drinking Water standards (EHCW) [54] standards (Table 7). The concentration of these pollutants exists in risky levels. The concentration of PO₄⁻ in the groundwater ranges from 0.097 to 53.23 mg/l while NO₃⁻ concentration ranges from 5.17 to 83.65 mg/l (Table 7 & Figure 6). Figure 6 shows that the northeastern part is more polluted than the southern part of the QAWT. This may attribute to the shallow depth to water, flood irrigation system, over use of the fertilizers and bad drainage system characterizing to the northeastern cultivated lands.

Table-7. Results of chemical analysis of the minor and trace elements in the surface and groundwater of the QAWT (values in mg/l).

| Element | Concentration range in surface water (mg/l) | Concentration range in ground water (mg/l) | World Health Organization Standards for Drinking Water (WHO) [53] (Acceptable) | Egyptian Health Committee for drinking Water standards (EHCW) [54] (Permissible) |
|-----------|---|--|--|--|
| Al | 0.1 - 0.4744 | (BDL) | 0.05 - 0.2 | 0.2 |
| B | 0.006 - 9.245 | 0.0607 - 3.369 | 1 | No index |
| Cd | (BDL) | (BDL) | - | - |
| Co | (BDL) | (BDL) | - | - |
| Cr | 0.004 - 0.0257 | 0.004 - 0.0308 | 0.01 - 0.1* | - |
| Cu | 0.02 - 0.0915 | 0.02 - 0.2293 | 1 | 1.5 |
| Fe | 0.003 - 0.2524 | 0.003 - 0.509 | 0.3 | 1 |
| Mn | 0.0149 - 0.0151 | 0.0062 - 0.2087 | 0.1 | 0.5 |
| Mo | 0.01 - 0.1584 | 0.01 - 0.0646 | 0.05 - 0.5* | - |
| Ni | 0.006 - 0.0114 | 0.006 - 0.0114 | 0.01 - 0.04* | - |
| Pb | (BDL) | (BDL) | - | - |
| Sr | 0.4252 - 22.425 | 0.4136 - 7.925 | 0.11* | - |
| V | 0.007 - 2.681 | 0.0438 - 0.4084 | 0.01 - 0.1 | - |
| Zn | 0.001 - 0.2257 | 0.012 - 0.1551 | 5 | 15 |
| Phosphate | 0.037 - 2.9 | 0.097 - 53.23 | 1 | 1 |
| Nitrate | 0.115 - 58.222 | 5.17 - 83.65 | 10 | 10 |

BDL is Below Detection Limit, and the sign * represents the median concentration [21].

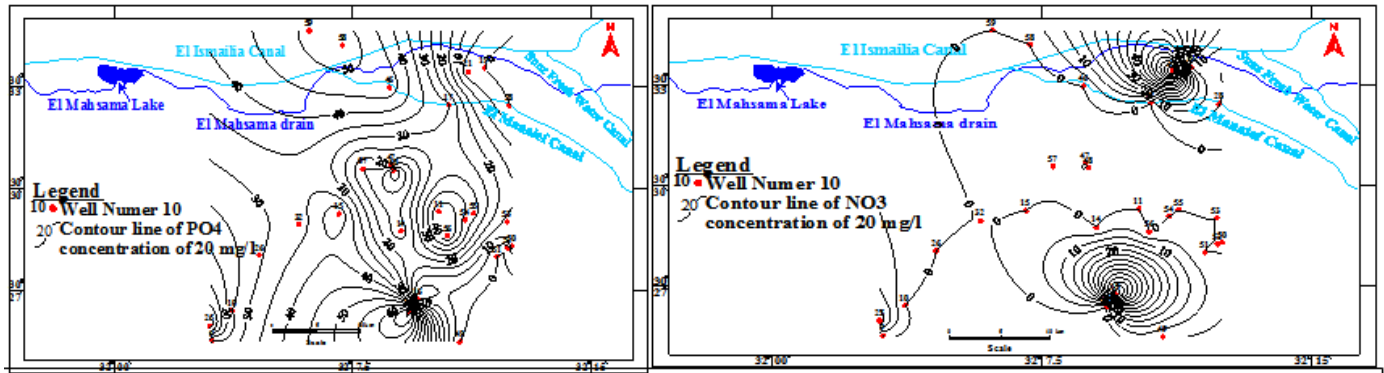


Figure-6. Iso-PO₄ concentration map (left) and Iso-NO₃ concentration map in mg/l (right) in the groundwater of the QAWT at 2005

In addition, the calculated GOD vulnerability index ranges from 0.2 (low vulnerable) to 0.5 (moderate vulnerable) (Table 8) while it ranges from 36 (low vulnerable) to 97 (very high) for PRAST index (Table 9). The calculated DRASTIC vulnerability index shows a range from 80 to 142 (Table 10). As a general, these indexes do not provide absolute answers; they only differentiate highly vulnerable areas from less vulnerable areas. The nature of these models are additive. Every parameter in the model has a fixed weight indicating the relative influence of the parameter in transporting contaminants to groundwater. The parameter rates are variable, which allows the user to calibrate the model to suit a given region. The vulnerability classes are defined according to the range of the obtained vulnerability index, taking into account a classification made by Navulur and Engel [55], but even the classification proposed by Lobo Ferreira and Oliveira [56] will show the same vulnerability in the QAWT.

Table-8. The estimated GOD index (GI) required for intrinsic vulnerability mapping of the QAWT

| W. N | G | O | D | GI | W. N | G | O | D | GI | W. N | G | O | D | GI | W. N | G | O | D | GI |
|------|---|-----|-----|------|------|---|-----|-----|------|------|---|-----|-----|------|------|---|-----|---|-----|
| 9 | 1 | 0.4 | 0.5 | 0.2 | 12 | 1 | 0.5 | 0.5 | 0.25 | 61 | 1 | 0.4 | 0.6 | 0.24 | 71 | 1 | 0.4 | 1 | 0.2 |
| 10 | 1 | 0.4 | 0.5 | 0.2 | 13 | 1 | 0.5 | 0.5 | 0.25 | 62 | 1 | 0.5 | 0.5 | 0.25 | 72 | 1 | 0.4 | 1 | 0.3 |
| 17 | 1 | 0.5 | 0.7 | 0.35 | 49 | 1 | 0.5 | 0.5 | 0.25 | 63 | 1 | 0.5 | 0.6 | 0.3 | 73 | 1 | 0.4 | 1 | 0.2 |
| 19 | 1 | 0.4 | 0.9 | 0.36 | 50 | 1 | 0.5 | 0.6 | 0.3 | 64 | 1 | 0.5 | 0.6 | 0.3 | 74 | 1 | 0.4 | 1 | 0.3 |
| 21 | 1 | 0.4 | 0.8 | 0.32 | 51 | 1 | 0.4 | 0.5 | 0.2 | 65 | 1 | 0.4 | 0.6 | 0.24 | 75 | 1 | 0.5 | 1 | 0.4 |
| 25 | 1 | 0.5 | 0.5 | 0.25 | 52 | 1 | 0.4 | 0.6 | 0.24 | 66 | 1 | 0.5 | 0.7 | 0.35 | 76 | 1 | 0.4 | 1 | 0.3 |
| 32 | 1 | 0.4 | 0.5 | 0.2 | 53 | 1 | 0.4 | 0.6 | 0.24 | 67 | 1 | 0.5 | 0.8 | 0.4 | 77 | 1 | 0.5 | 1 | 0.4 |
| 47 | 1 | 0.5 | 0.6 | 0.3 | 54 | 1 | 0.4 | 0.6 | 0.24 | 58 | 1 | 0.5 | 0.7 | 0.35 | 78 | 1 | 0.4 | 1 | 0.3 |
| 48 | 1 | 0.5 | 0.6 | 0.3 | 55 | 1 | 0.4 | 0.6 | 0.24 | 59 | 1 | 0.4 | 0.8 | 0.32 | 79 | 1 | 0.5 | 1 | 0.4 |
| 28 | 1 | 0.5 | 0.7 | 0.35 | 56 | 1 | 0.4 | 0.6 | 0.24 | 68 | 1 | 0.5 | 35 | 17.5 | 80 | 1 | 0.4 | 1 | 0.4 |
| 46 | 1 | 0.4 | 0.8 | 0.32 | 57 | 1 | 0.5 | 0.5 | 0.25 | 69 | 1 | 0.5 | 0.6 | 0.3 | 81 | 1 | 0.5 | 1 | 0.5 |
| 11 | 1 | 0.5 | 0.5 | 0.25 | 60 | 1 | 0.5 | 0.6 | 0.3 | 70 | 1 | 0.4 | 0.8 | 0.32 | 82 | 1 | 0.4 | 1 | 0.4 |

Table-9. The estimated PRAST index (PI) required for intrinsic vulnerability mapping of the QAWT

| W.N | P | R | A | S | T | PI | W.N | P | R | A | S | T | PI | W.N | P | R | A | S | T | PI |
|-----|----|---|----|----|----|----|-----|----|---|----|----|----|----|-----|----|---|----|----|----|----|
| 9 | 4 | 1 | 6 | 25 | 0 | 36 | 51 | 16 | 1 | 9 | 25 | 0 | 51 | 59 | 10 | 1 | 18 | 30 | 15 | 74 |
| 10 | 4 | 1 | 9 | 25 | 0 | 39 | 52 | 16 | 1 | 6 | 25 | 0 | 48 | 68 | 10 | 1 | 9 | 30 | 15 | 65 |
| 17 | 22 | 1 | 6 | 25 | 0 | 54 | 53 | 16 | 1 | 9 | 25 | 0 | 51 | 69 | 10 | 1 | 24 | 30 | 15 | 80 |
| 19 | 26 | 1 | 9 | 25 | 0 | 61 | 54 | 18 | 1 | 12 | 25 | 0 | 56 | 70 | 16 | 1 | 9 | 25 | 15 | 66 |
| 21 | 24 | 1 | 6 | 25 | 16 | 56 | 55 | 18 | 1 | 6 | 25 | 0 | 50 | 71 | 24 | 1 | 9 | 25 | 15 | 74 |
| 25 | 4 | 1 | 9 | 25 | 16 | 55 | 56 | 16 | 1 | 9 | 25 | 0 | 51 | 72 | 10 | 1 | 9 | 25 | 15 | 60 |
| 32 | 24 | 1 | 24 | 25 | 16 | 90 | 57 | 16 | 1 | 12 | 25 | 17 | 54 | 73 | 10 | 1 | 12 | 30 | 15 | 68 |
| 47 | 14 | 1 | 12 | 25 | 16 | 68 | 60 | 4 | 1 | 18 | 25 | 17 | 65 | 74 | 10 | 1 | 18 | 30 | 15 | 74 |
| 48 | 14 | 1 | 6 | 25 | 15 | 62 | 61 | 4 | 1 | 12 | 25 | 16 | 59 | 75 | 10 | 1 | 9 | 30 | 15 | 65 |
| 28 | 30 | 1 | 9 | 25 | 15 | 80 | 62 | 6 | 1 | 9 | 25 | 16 | 57 | 76 | 32 | 1 | 6 | 30 | 15 | 84 |
| 46 | 14 | 1 | 12 | 25 | 15 | 67 | 63 | 8 | 1 | 6 | 35 | 16 | 66 | 77 | 10 | 1 | 9 | 35 | 15 | 70 |
| 11 | 16 | 1 | 18 | 25 | 15 | 75 | 64 | 36 | 1 | 9 | 35 | 16 | 97 | 78 | 14 | 1 | 6 | 35 | 15 | 71 |
| 12 | 8 | 1 | 18 | 25 | 15 | 67 | 65 | 6 | 1 | 12 | 35 | 16 | 70 | 79 | 14 | 1 | 9 | 35 | 16 | 74 |
| 13 | 8 | 1 | 9 | 25 | 15 | 58 | 66 | 8 | 1 | 18 | 35 | 16 | 78 | 80 | 12 | 1 | 12 | 35 | 16 | 76 |
| 49 | 6 | 1 | 12 | 25 | 15 | 59 | 67 | 8 | 1 | 9 | 30 | 16 | 64 | 81 | 8 | 1 | 18 | 35 | 16 | 78 |
| 50 | 16 | 1 | 18 | 25 | 0 | 75 | 58 | 10 | 1 | 12 | 25 | 15 | 64 | 82 | 10 | 1 | 24 | 35 | 16 | 86 |

Table-10. The estimated DRASTIC Index (DI) required for intrinsic vulnerability mapping of the QAWT

| W. N | D | R | A | S | T | I | C | DI | W. N | D | R | A | S | T | I | C | DI |
|------|----|---|----|----|----|----|----|-----|------|----|---|----|----|----|----|---|-----|
| 9 | 35 | 1 | 6 | 25 | 0 | 15 | 3 | 85 | 61 | 35 | 1 | 12 | 25 | 16 | 10 | 3 | 102 |
| 10 | 35 | 1 | 9 | 25 | 0 | 15 | 3 | 88 | 62 | 35 | 1 | 9 | 25 | 16 | 10 | 3 | 99 |
| 17 | 40 | 1 | 6 | 25 | 0 | 15 | 3 | 90 | 63 | 35 | 1 | 6 | 35 | 16 | 10 | 3 | 106 |
| 19 | 40 | 1 | 9 | 25 | 0 | 15 | 6 | 96 | 64 | 40 | 1 | 9 | 35 | 16 | 15 | 3 | 119 |
| 21 | 40 | 1 | 6 | 25 | 16 | 10 | 6 | 104 | 65 | 35 | 1 | 12 | 35 | 16 | 15 | 3 | 117 |
| 25 | 35 | 1 | 9 | 25 | 16 | 10 | 6 | 102 | 66 | 40 | 1 | 18 | 35 | 16 | 15 | 3 | 128 |
| 32 | 35 | 1 | 24 | 25 | 16 | 10 | 12 | 123 | 67 | 45 | 1 | 9 | 30 | 16 | 15 | 3 | 119 |
| 47 | 35 | 1 | 12 | 25 | 16 | 10 | 6 | 105 | 58 | 40 | 1 | 12 | 25 | 15 | 10 | 3 | 106 |
| 48 | 35 | 1 | 6 | 25 | 15 | 10 | 12 | 104 | 59 | 40 | 1 | 18 | 30 | 15 | 10 | 3 | 117 |
| 28 | 40 | 1 | 9 | 25 | 15 | 30 | 6 | 126 | 68 | 35 | 1 | 9 | 30 | 15 | 10 | 3 | 103 |
| 46 | 40 | 1 | 12 | 25 | 15 | 30 | 12 | 135 | 69 | 35 | 1 | 24 | 30 | 15 | 10 | 6 | 121 |
| 11 | 35 | 1 | 18 | 25 | 15 | 15 | 6 | 115 | 70 | 40 | 1 | 9 | 25 | 15 | 10 | 6 | 106 |
| 12 | 35 | 1 | 18 | 25 | 15 | 15 | 6 | 115 | 71 | 35 | 1 | 9 | 25 | 15 | 10 | 6 | 101 |
| 13 | 35 | 1 | 9 | 25 | 15 | 15 | 6 | 106 | 72 | 40 | 1 | 9 | 25 | 15 | 10 | 6 | 106 |
| 49 | 35 | 1 | 12 | 25 | 15 | 15 | 3 | 106 | 73 | 35 | 1 | 12 | 30 | 15 | 10 | 6 | 109 |
| 50 | 35 | 1 | 18 | 25 | 0 | 15 | 3 | 97 | 74 | 45 | 1 | 18 | 30 | 15 | 10 | 6 | 125 |
| 51 | 35 | 1 | 9 | 25 | 0 | 15 | 3 | 88 | 75 | 40 | 1 | 9 | 30 | 15 | 10 | 6 | 111 |

Continue

| | | | | | | | | | | | | | | | | | |
|----|----|---|----|----|----|----|---|-----|----|----|---|----|----|----|----|---|-----|
| 52 | 35 | 1 | 6 | 25 | 0 | 15 | 3 | 85 | 76 | 35 | 1 | 6 | 30 | 15 | 10 | 6 | 103 |
| 53 | 35 | 1 | 9 | 25 | 0 | 10 | 3 | 83 | 77 | 40 | 1 | 9 | 35 | 15 | 10 | 6 | 116 |
| 54 | 35 | 1 | 12 | 25 | 0 | 10 | 3 | 86 | 78 | 40 | 1 | 6 | 35 | 15 | 10 | 6 | 113 |
| 55 | 35 | 1 | 6 | 25 | 0 | 10 | 3 | 80 | 79 | 45 | 1 | 9 | 35 | 16 | 10 | 6 | 122 |
| 56 | 35 | 1 | 9 | 25 | 0 | 10 | 3 | 83 | 80 | 45 | 1 | 12 | 35 | 16 | 10 | 6 | 125 |
| 57 | 35 | 1 | 12 | 25 | 17 | 10 | 3 | 103 | 81 | 45 | 1 | 18 | 35 | 16 | 10 | 6 | 131 |
| 60 | 35 | 1 | 18 | 25 | 17 | 10 | 3 | 109 | 82 | 50 | 1 | 24 | 35 | 16 | 10 | 6 | 142 |

W.N is well number, D is the Depth to water, R is the net Recharge, A is the Aquifer media, S is the Soil media, T is the Topography, I is the Impact of the vadose zone, C is the hydraulic Conductivity and DI is the vulnerability DRASTIC index.

The effect of the hydrogeological conditions on the vulnerability assessment of the QAWT is clear through the small differences between the produced intrinsic vulnerability maps applying the PRAST and DRASTIC methods of overlay and index. The final intrinsic vulnerability maps obtained in this study show three classes of vulnerability in the QAWT: low, medium and high (Figure 7, 8 and 9). The resulted intrinsic vulnerability map of QAWT applying GOD method (Figure 7) indicates higher vulnerability in the area around El-Mahsama lake and El-Mahsama drain and clearly indicates the bad drainage system of this locality. The same results of high vulnerable areas of the QAWT are obtained applying both PRAST and DRASTIC models (Figure 8 & 9). These two vulnerability maps reflect simplicity of aquifer vulnerability spatial distribution which is practically more or less not true. This may attribute to the selection of the ratings and weights that has to be assigned to the five or seven base maps which represent the five or seven parameters in case of PRAST or DRASTIC model. Such a selection can strongly affect the result of the final vulnerability map. Given the fact that it is not possible to avoid subjectivity, the way to deal with it is by performing a sensitivity analysis which is out of scope of this study.

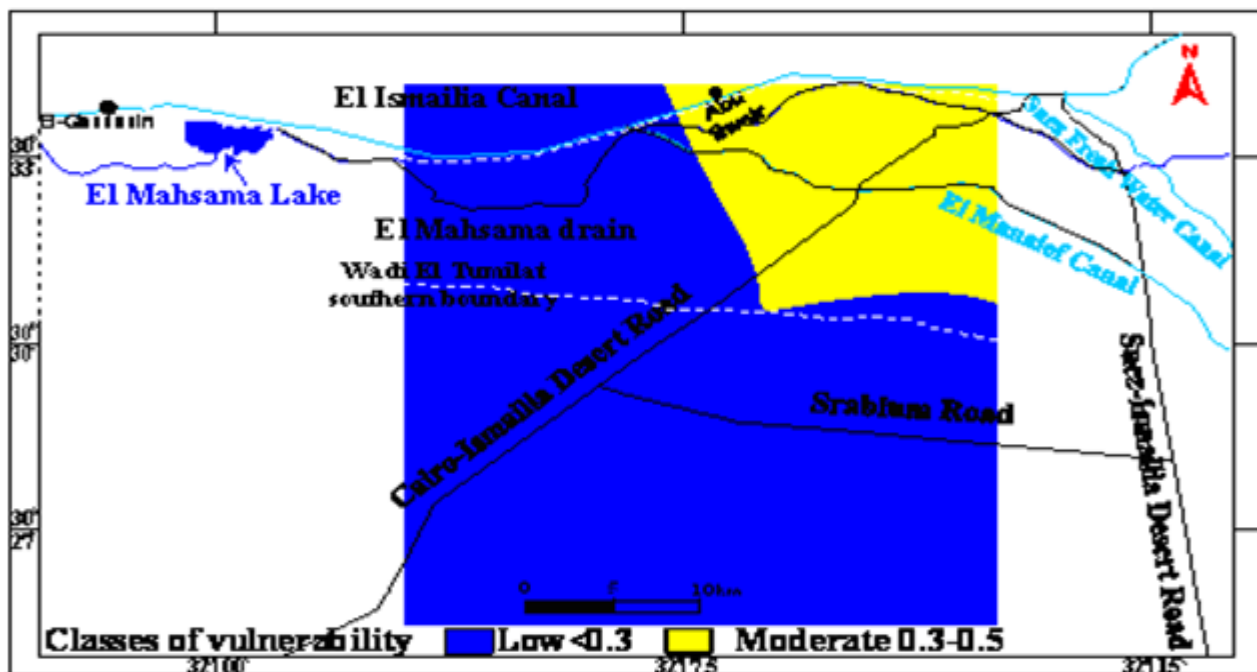


Figure-7. Intrinsic vulnerability map according to GOD method

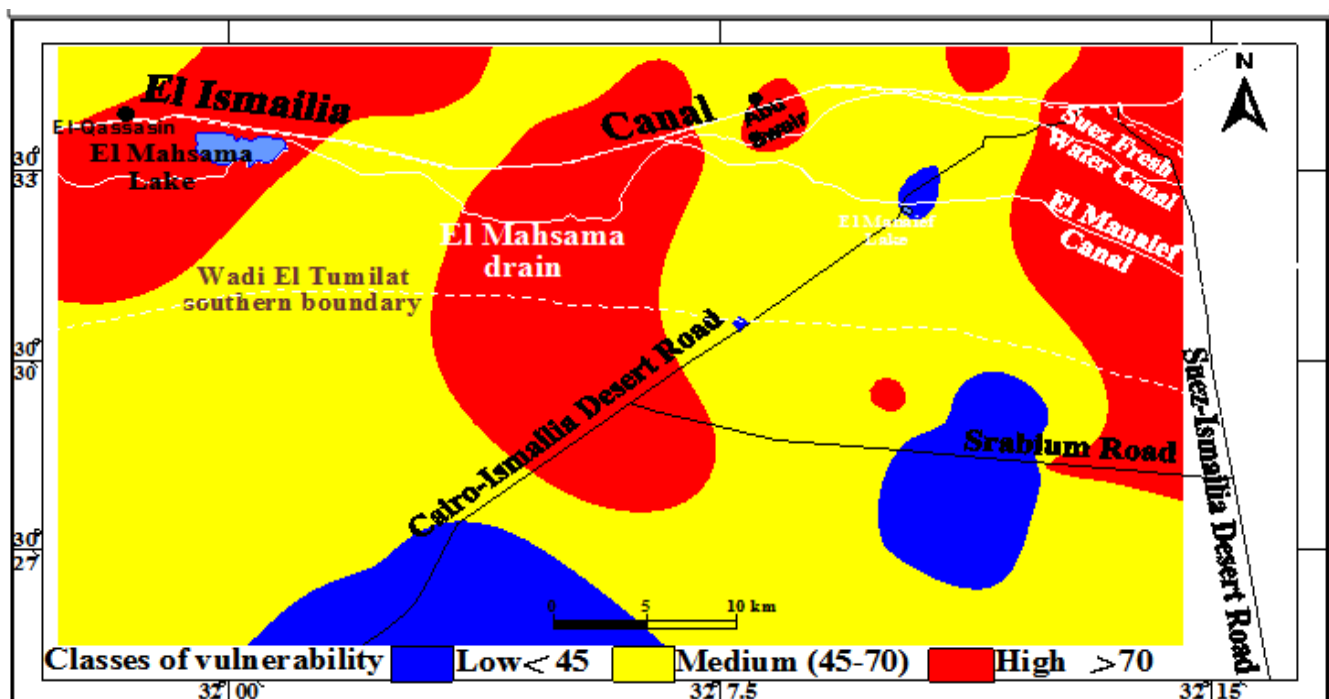


Figure-8. Intrinsic vulnerability map according to PRAST method

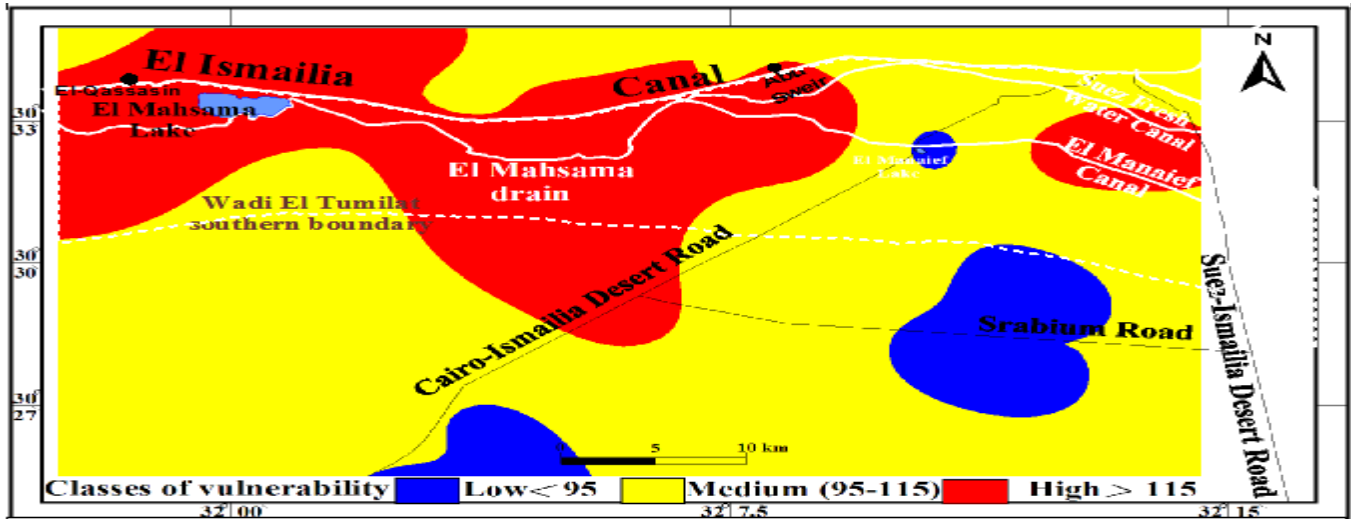


Figure-9. Intrinsic vulnerability map according to DRASTIC method

The obtained vulnerability maps by different methods show, in general terms, some sort of homogeneity in respect to overall zonation. In other words, the maps show two distinct zones, the northern zone which tends to attain comparatively high index values, and the southern zone which is characterized generally by the lowest index values. This is particular due mainly to the extreme difference between the northern and the southern zones in respect to depth to water, net rate of recharge, topography and presence or absence of agricultural lands where pesticides weights has to be taken into account. The northern zone is featured by lands of relatively low levels and accordingly the proximity of groundwater to the surface, in addition to intensive irrigation. The southern zone is characterized by higher topographic levels accompanied accordingly by deeper groundwater in addition to limited irrigation practice. Therefore, it can be stated that the southern zone is less vulnerable than the northern zone.

As a general, the obtained results related to the vulnerability show the high extension of the zones with medium vulnerability (21%, 65% and 61% for applying GOD, PRAST and DRASTIC methods respectively) comparing to the other zones of the groundwater. The zones with high vulnerability occupy about 35% and 31% from applying PRAST and DRASTIC methods respectively while the GOD method do not show any ratio for this class. The zones with low vulnerability occupy about 79%, 13% and 8% of the total surface of the groundwater in case of applying GOD, PRAST and DRASTIC methods respectively. The zones with high vulnerability are located mainly in spots between El-Qassasin and El-Mahsama lake in the west and El-Manaif village in the east. Also, they cover great parts of Abu Sweir city (Al-Amal and Al-Mostaqbal new towns). The high vulnerability in these zones is mainly related to the low values of depth to water (less than 10 m), the high permeability of the soils (9 m/day) and the high permeability of the vadose zone materials (more than 11 m/day), which are mainly constituted by sandstone or by intercalations of sand and sandstone. The moderate vulnerability areas are locating in a vast zone located in the south, west and north of the Ismailia town. Other occurrence is related to the area of the village of Nefisha, at the crossroads of the Cairo-Ismailia and Suez-Ismailia highways, and in the zone of Sarabium. Finally, the areas with low vulnerability are locating in the extreme south of the Wadi El-Tumilat, and in some restricted zones NE the 10th of Ramadan city and in the region of the El-Wadi drain. However, these newly developed maps are found to be more or less in conformity with the salinity distribution map of the groundwater in the study area (Figure 5), which shows high values of TDS in the north and that the salinity decreases towards the south direction. Also, the developed maps shows the presence of two infected centers with pollution (in the north and the south) which is comparable with the PO_4^- & NO_3^- concentration contour maps (Figure 6). Finally, it is noticed that in general, in the QAWT, the areas located adjacent to the Ismailia canal and local drains crossing high vulnerable zones are characterized by a permeable vadose zone, and that can increase the risk of the pesticides' pollution and other pollutants in these areas.

In the other point, if the newly developed DRASTIC map is compared with the previous DRASTIC maps prepared by RIGW/IWACO [37] (Figure 10) and by Saad [39] (Figure 11) and by the vulnerability map of Dahab, et al. [40] (based on the classification scheme of Zekster [57] (Figure 12), some distinct variations are observed. Whereas, the newly developed DRASTIC map identifies spots of the northern portion of the QAWT as highly vulnerable, and the southern portion attains low vulnerability, the other previous maps reveal opposite conclusions. This is, however, due mainly to the fact that the latter vulnerability mapping do not take into consideration some important factors (depth to water, net recharge and hydraulic conductivity). RIGW/IWACO [37] DRASTIC map neglects the soil media and hydraulic conductivity parameters while [37] DRASTIC map divides the DRASTIC parameters into static (five parameters) and dynamic (two parameters). Dahab, et al. [40] vulnerability map neglects the depth to groundwater and the net recharge parameters. Also, the RIGW/IWACO [37] map has not given differentiation between the weights of the various factors involved in the aquifer vulnerability, and accordingly, all factors are given the same degree of importance. It can thus be concluded that the RIGW/IWACO [37] map represents, to a great extent, the static features, of the aquifer vulnerability. Accordingly, if the dynamic parameters are integrated to the RIGW/IWACO [37] map the final aquifer vulnerability will approach the final DRASTIC map presented in this paper. Finally, these previous maps are considered as operative maps in the classification of Civita [43].

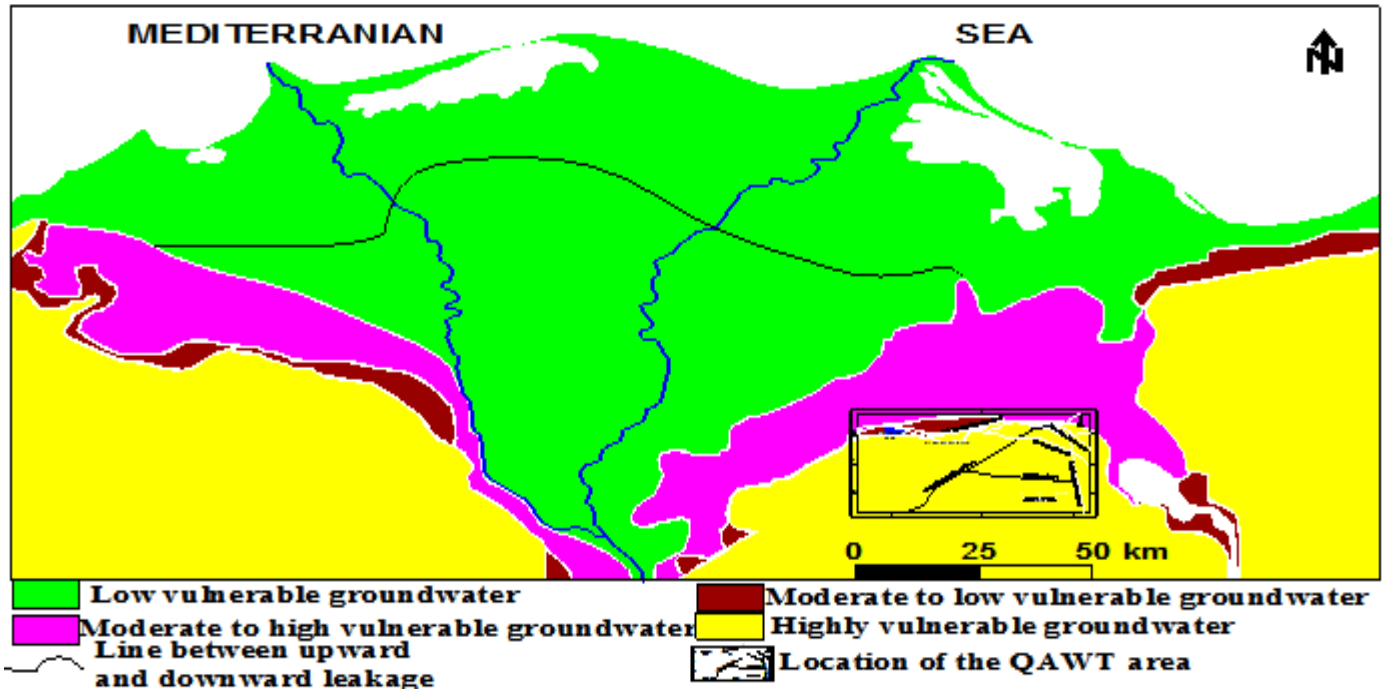


Figure-10. Intrinsic vulnerability map according to DRASTIC method (after RIGW/IWACO [37])

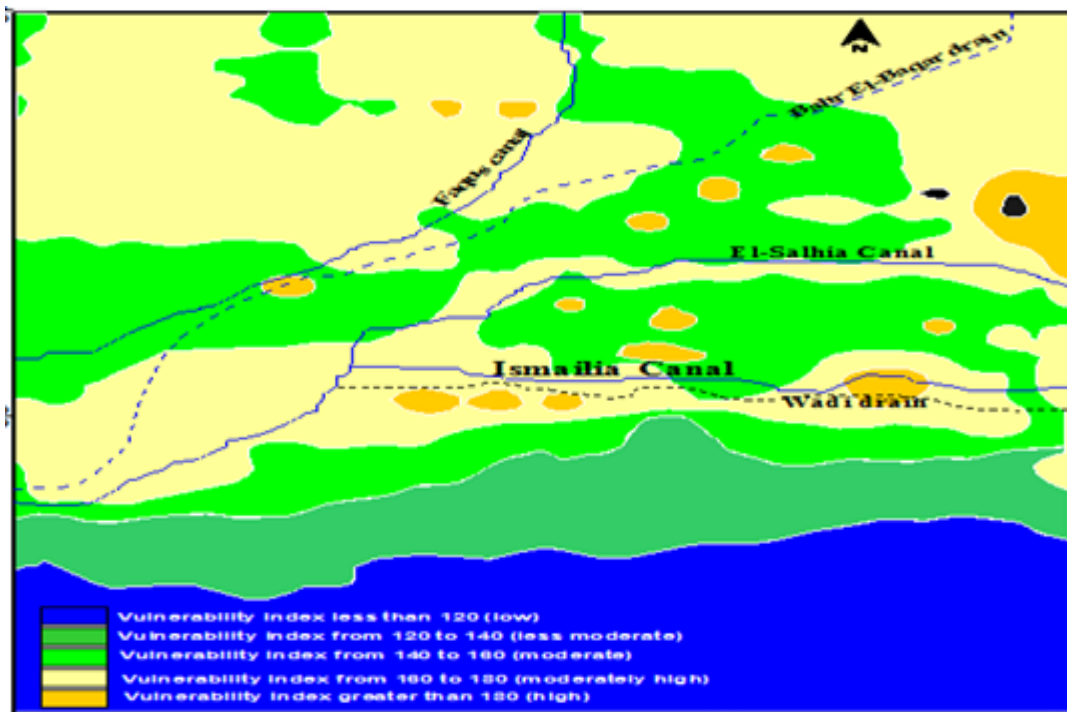


Figure-11. Intrinsic vulnerability map according to DRASTIC method (after Saad [39])

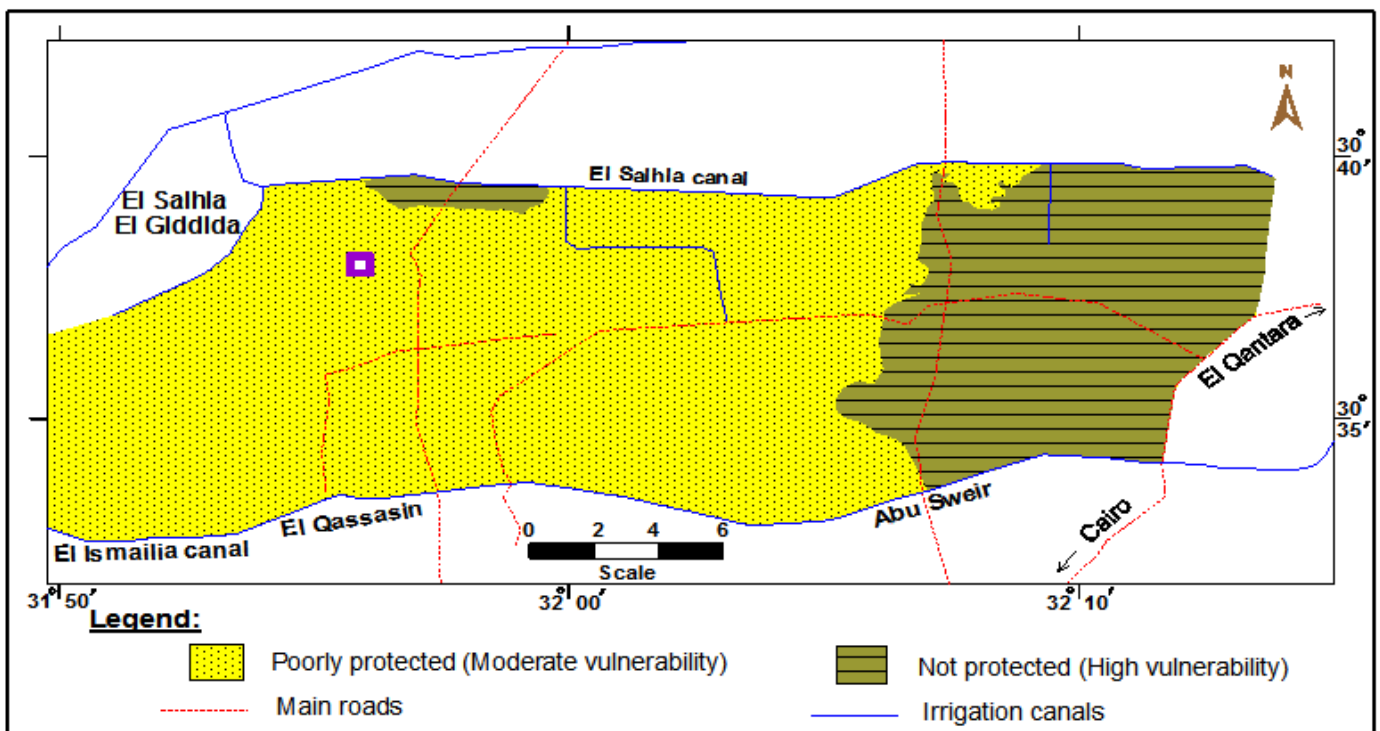


Figure-12. Intrinsic vulnerability map according to DRASTIC method (after Dahab, et al. [40])

4. Conclusion and Recommendations

In this paper, the groundwater pollution of the QAWT is detected from the results of the chemical analysis of both surface and groundwater samples collected at 2005. Both surface and groundwater resources are mostly polluted with B, Sr, V, PO_4^- and NO_3^- with risky levels. The concentration of PO_4^- and NO_3^- in the groundwater ranges from 0.097 to 53.23 and 5.17 to 83.65 ppm respectively. The northeastern part is more polluted than the southern part of the QAWT due to shallow depth to water, flood irrigation system, over use of the fertilizers and bad drainage system.

Three different overlay and index methods (GOD, PRAST and DRASTIC) have been used based on the hydrogeological conditions for vulnerability assessment. The calculated vulnerability indexes resulted from these three methods show great differences due to the different criteria used. The calculated GOD vulnerability index ranges from 0.2 (low vulnerable) to 0.5 (moderate vulnerable) while it ranges from 36 (low vulnerable) to 97 (very high vulnerable) for PRAST index, and from 80 (low vulnerable) to 142 (very high vulnerable) for DRASTIC index. These indexes only differentiated highly vulnerable areas from less vulnerable areas. Also, a modification from weight of 1 to 2 for the DRASTIC criterion relative to the slope of topography is assumed to adequate the hydrogeological conditions of arid zones like the QAWT.

The obtained results related to the vulnerability maps show the high extension of the zones with medium vulnerability (21%, 65% and 61% for applying GOD, PRAST and DRASTIC method respectively) comparing to the other zones of the groundwater. The zones with high vulnerability occupy about 35% for the PRAST overlay method and 31% for the DRASTIC overlay method while the GOD method do not show any ratio for this class. The zones with low vulnerability occupy about 79% for the GOD overlay method, 13% and 8% of the total surface of the groundwater in case of applying PRAST and DRASTIC overlay methods. The zones with high vulnerability are located mainly in spots between El-Qassasin and El-Mahsama lake in the west and El-Manaif village in the east. Also, they cover great parts of El-Manaif village in the east and Abu Sweir city (Al-Amal and Al-Mostaqbal new towns). The high vulnerability in these zones is mainly related to the low values of depth to water (less than 10 m), the high soil permeability (9 m/day) and the high permeability of the vadose zone materials (more than 11 m/day). The developed intrinsic vulnerability maps show the presence of two infected centers with pollution (in the north and the south) which are comparable with the PO_4^- & NO_3^- concentration contour maps. The newly developed DRASTIC map is more or less comparable with the previous DRASTIC maps cited in RIGW/IWACO [37] and Saad [39] and the vulnerability map in Dahab, et al. [40]. Some distinct variations are observed due mainly to both the fact that the latter vulnerability mapping do not use some important factors like depth to water, net recharge and hydraulic conductivity, and equalization between the weights of the various factors involved in preparing these aquifer vulnerability maps.

Based on the results of this paper, it is recommended that the most suitable areas for new reclamation activity locate in the southern boundary of Wadi El Tumilat especially the strip south El Mahsama drain by 5 km. It is also highly recommended to make public awareness about the threats of pollution on groundwater resources especially in the vulnerable areas. Sealing the drainage system to minimize the pollution by heavy and trace elements in the northern and eastern lowlands is highly recommended. Improving the irrigation system and preventing the continuous drainage of sewage and waste water to Ismailia canal and the drainage system is also recommended. The continuous use of the huge garbage dumps, especially near Sarabium area and the Ismailia-Suez desert road characterized by shallow groundwater must be transported to other suitable places.

References

- [1] J. Margat, *Vulnerabilite des nappes d'eau souterraine a la pollution*: BRGM Publication 68 SGL 198 HYD, Orleans.Guideline for Groundwater Vulnerability Mapping Doc, 1968.
- [2] E. F. Vowinkel, R. M. Clawges, D. E. Buxton, D. A. Stedfast, and J. B. Louis, "Vulnerability of public drinking water supplies in New Jersey to pesticides," U.S. Geological Survey, Fact Sheet FS-165-96. Reston/USA, p. 3, 1996.
- [3] J. Vrba and A. Zaporozec, "Guidebook on mapping groundwater vulnerability, international association of hydrogeologists (IAH)," International Contribution to Hydrogeology, v. 16, Hannover: Heise Verlag, 1994.
- [4] A. A. Shata, "Geological structure of the Nile Delta," *Journ. of Engin. Cairo, (In Arabic)*, pp. 1-3, 1965.
- [5] I. F. El Fayoumy, "Geology of groundwater supplies in the region East of the Nile Delta," Unpublished Ph. D. Thesis, Fac. Sci., Cairo Univ, 1968.
- [6] A. A. Shata and I. F. El Fayoumy, "Remarks on the regional geological structure of the Nile Delta," *Symposium Hydrology of Delta, UNESCO*, vol. 1, pp. 189-197, 1970.
- [7] E. M. El Shazly, M. A. Abdel Hady, M. M. El Shazly, M. A. El Ghawabby, I. A. El Kassas, A. B. Salman, and M. A. Morsi, "Geological and groundwater potential studies of El Ismailia master plan study area," Remote Sensing Research Project, Academy of Scientific Research and Technology, Cairo, Egypt, 1975.
- [8] M. E. El Diasty, "The aeromagnetic map of the Delta area and the interpretation of the geophysical data," Unpublished M. Sc. Thesis, Fac. Sc., Alex. Univ., Egypt, 1969.
- [9] S. A. Ahmed, "The geology of the desert east of Cairo," *Bull. Inst. Desert, Egypt*, vol. 111, pp. 42-89, 1977.
- [10] M. D. El Dairy, "Hydrogeological studies on the eastern part of Nile Delta using isotope techniques," Unpublished M. Sc. Thesis, Fac. of Sc., Zagazig Univ, 1980.
- [11] M. El Ahwani, "Geological and sedimentological studies of gabal shabrawet area, Suez canal district, Egypt," *Ann. Geol. Surv. Cairo.*, vol. 12, pp. 305-381, 1982.
- [12] E. A. Korany, E. H. Shendi, and S. Abdel Tawab, "Integrated detection of the problem of groundwater over-flow in Abu Zaabal Basalt Quarries, Egypt," E. G. S. Proc. of 11th Ann. Meet, 1993.
- [13] M. M. Gad, "Hydrogeological studies for groundwater reservoirs, East of the tenth of Ramadan city and vicinities," Unpublished M. Sc. Thesis, Ain Shams Univ, 1995.
- [14] I. Z. El Shamy and M. H. Geriash, "Hydrogeology of West Ismailia area, Egypt," *Desert Inst. Bull., Egypt*, vol. 42, pp. 271-288, 1991.
- [15] Z. El Shamy, "Hydrogeology of Wadi El Tumilat and surroundings, East of the Nile Delta, Egypt," 8th Symp. Phaner. Develop., Egypt, 1992.
- [16] H. M. G. Ismail, "Study the vulnerability of groundwater aquifer for pollution in Wadi El-Tumilat, Eastern Delta," Unpublished M.Sc. Thesis, Fac. of Sci., Cairo Univ, 2008.
- [17] C. A. Black, *Methods of soil analysis*. Madison: Am. Soc., Agron. Inc. Pub, 1973.
- [18] J. R. Philip, "The thory of infiltration. 1. The infiltration equation and its solution," *Soil Sci.*, vol. 83, pp. 345-457, 1957.

- [19] H. F. Afify, "Studies on the municipal contamination of water resources in some villages of ismailia governorate, Egypt," Unpublished Ph. D. Thesis, Suez Canal Univ., Egypt, 2004.
- [20] F. R. Rainwater and L. L. Thatcher, "Methods for collection and analysis of water samples, V.S.G.S. water supply, paper No. 1454," p. 301, 1960.
- [21] B. Holting, T. Haertle, K. H. Hohberger, K. H. Nachtigal, E. Villinger, W. Weinzierl, and J. P. Wrobel, "Konzept zur ermittlung der schutzfunktion der grundwasseruberdeckung," *Geol. Jahrbuch, Reihe C, Heft 63, Hannover*, 1995.
- [22] C. V. Theis, "The relation between the lowering of the piezometer surface and the rate and duration of discharge of well using groundwater storage," *Am. Geophys. Union Trans.*, vol. 16, pp. 512-524, 1935.
- [23] H. H. Cooper and C. E. Jacob, "A generalized graphical method for evaluating formation constants and summarizing well field history," *Am. Geophys. Union Trans.*, vol. 27, pp. 526-534, 1946.
- [24] A. A. Shata, "Genesis, formation and classification of the soils South Ismaelya canal between Belbeis and Ismaelya including Wadi El-Tumilat," M. Sc. Thesis, Fac. Agricul., Zagazig Univ, 1978.
- [25] A. Bodenkunde, *Bodenkundliche kartieranleitung*, 4th ed. Hannover, Germany: Schweizerbart Publ, 1994.
- [26] L. Aller, T. Bennett, J. H. Lehr, R. J. Petty, and G. Hackett, "Drastic: A standardized system for evaluating ground water pollution potential using hydrogeological settings," EPA Reports, 600/2-87-035, Washington DC, USA, 1987.
- [27] S. S. D. Foster, "Fundamental concepts in aquifer vulnerability, pollution risk and protection strategy," *Vulnerability of Soil and Groundwater to Pollutants*; 38 (Van Duijvenboden & H.G. Van Waegeningh eds.), TNO Commission on Hydro Res, Proc. and Inform., Hague, 1987, pp. 69-86.
- [28] N. Robins, B. Adams, S. Foster, and R. Palmer, "Groundwater vulnerability mapping: The British perspective," *Hydrogeologie*, vol. 3, pp. 35-42, 1994.
- [29] S. S. D. Foster, *Groundwater recharge and pollution vulnerability of British aquifers – a critical overview*. London, UK: Geological Society Special Publication, 13, 1997.
- [30] N. Doerfliger, P. Y. Jeannin, and F. Zwahlen, "Water vulnerability assessment in karst environments: A new method of defining protection areas using a multi-attribute approach and GIS tools (EPIK Method)," *Environmental Geology*, vol. 39, pp. 165-176, 1999.
- [31] S. Hannapel and H. J. Voight, "Vulnerability maps as a tool for groundwater protection – case studies from Eastern Germany," *Hydrogeology and Land use Management* (M. Fendekova & M. Fendek eds.), Proc. XXIX Congress IAH Bratislava, 1999, pp. 59-64.
- [32] R. C. Gogu and A. Dassargues, "Current trends and future challenges in groundwater vulnerability assessment using overlay and index methods," *Environmental Geology*, vol. 39, pp. 549-559, 2000.
- [33] T. Al Zabet, "Evaluation of aquifer vulnerability to contamination potential using the drastic method," *Environmental Geol.*, vol. 43, pp. 203-208, 2002.
- [34] D. Daly, A. Dassargues, D. Drew, S. Dunne, N. Goldscheider, S. Neale, I. C. Popescu, and F. Zwahlen, "Main concepts of the European approach to karst-groundwater-vulnerability assessment and mapping," *Hydrogeology Journal*, vol. 10, pp. 340-345, 2002.
- [35] S. Foster, R. Hirata, D. Gomes, M. D'Elia, and M. Paris, *Groundwater quality protection. A guide for water utilities, municipal authorities and environment agencies*. Washington, DC: The World Bank, 2002.
- [36] A. Zurek, S. Witczak, and R. Duda, "Vulnerability assessment in fissured aquifers. In: Groundwater quality and vulnerability," *Prace Wydzialu Nauko Ziemi*, 22, (Rubin, Rubin & Witkowski eds.), Univ. of Silesia, Sosnowiec (in Polish), 2002.
- [37] RIGW/IWACO, *Vulnerability of groundwater to pollution*. Cairo, Egypt, 1990.
- [38] RIGW, "Groundwater potential in the Nile valley and Delta," Internal Report. Cairo, Egypt, 1991.
- [39] A. K. F. Saad, "Environmental hydrogeologic impacts of groundwater withdrawal in the Eastern Nile Delta region with emphasis on ground-water pollution potential," Unpublished Ph.D Thesis, Institute for Environmental Studies and Research, Ain Shams Univ, 1998.
- [40] K. A. Dahab, E. A. El Abd, M. K. Fattah, and M. M. El Osta, "Assessment of groundwater problems of the quaternary aquifer in the area between El Salhyia El Gidida-Abu Sweir, East Nile Delta, Egypt," *GRMENA II*, vol. 2007, pp. 329-353, 2007.
- [41] S. S. D. Foster and R. A. Hirata, *Groundwater pollution risk assessment—a methodology using available data*. Lima, Peru: WHO-PAHO-CEPIS Publication, 1988.
- [42] N. Goldscheider and C. Popescu, *The European approach. In: Zwahlen F (Ed) vulnerability and risk mapping for the protection of carbonate (Karst) aquifers*. Brussels: European Commission, 2004.
- [43] M. Civita, *Le carte della vulnerabilita degli acquiferi all inquinamento: Teoria e pratica*. Bologna, Italy: Pitagora Editrice, 1994.
- [44] United States Environmental Protection Agency (US EPA), "PRZM-2, a model for predicting pesticide fate in the crop root and unsaturated soil zones: User manual for release 2.0. U.S. Environmental protection agency, EPA 600/R-93/045," p. 406, 1993.
- [45] L. Aller, T. Bennett, J. H. Lehr, and R. J. Petty, "Drastic standardized system for evaluation groundwater pollution using hydrogeologic settings," U.S. EPA Robert S., Kerr Environmental Research Laboratory, Oklahoma, EPA/600/2-85, 1985.
- [46] D. S. Durnford, K. R. Thompson, D. A. Ellerbrook, J. C. Loftis, and G. S. Davies, "Screening methods for ground water pollution potential from pesticide use in Colorado agriculture," Colorado Water Resources Research Institute, Completion Report No. 157. Fort Collins, 1990.
- [47] J. P. Lobo Ferreira and M. M. Oliveira, "Drastic ground water vulnerability mapping of Portugal," Proceedings from the 27th Congress of the International Association for Hydraulic Research, San Francisco, USA, Aug. 10-15, 1997, pp. 132-137.
- [48] S. D. Lynch, A. G. Reynders, and R. E. Schulze, "A drastic approach to ground water vulnerability in South Africa," *South African Journal of Science*, vol. 93, pp. 59-60, 1997.
- [49] M. Melloul and M. Collin, "A proposed index for aquifer water-quality assessment, the case of Israel's Sharon region," *Journal of Environmental Management*, vol. 54, pp. 131-142, 1998.
- [50] Y. J. Kim and S. Hamm, "Assessment of the potential for ground water contamination using the DRASTIC/EGIS technique, Cheongju area, South Korea," *Hydrogeology Journal*, vol. 7, pp. 227-235, 1999.
- [51] S. Lyakhloufi, S. Er-Rouane, N. Ouazzani, and A. EL Habil, "Vulnerabilite et rique de pollution de la nappe phreatique du haouz de marrakech," *Hydrogeologie, Orleans*, vol. 3, pp. 43-52, 1999.
- [52] E. M. Fatouh, M. I. GAD, A. A. Abdel-Baki, and M. A. Awad, "Water resources characteristics between 10th of Ramadan city and Suez canal area, Egypt," Proceedings of the 6th Int. Engineering Conference Fac., of Eng.-Mansoura Univ., Mansoura/Sharm El-Sheikh March 2008 20-23, 2008, pp. 290-301.
- [53] World Health Organization Standards for Drinking Water (WHO), *International Standards for drinking water*, 3rd ed. vol. 1. Geneva, Switzerland, 1984.
- [54] Egyptian Health Committee for drinking Water standards (EHCW), "المنزلي والاسد تعمال الشرب لمياه المصرية المعايير", 1995. "للمياه العامة المواردت نظيم شأن في 1978 لسنة 27 رقم ط بقلا لقا دون".
- [55] K. C. S. Navulur and B. Engel, "Predicting spatial distributions of vulnerability of Indiana State aquifer system to nitrate leaching using GIS." Available: http://www.ncgia.ucsb.edu/conf/SANTA_FE_CD-ROM/sfpapers/navulurkumar/my_paper.html, 1997.
- [56] J. P. Lobo Ferreira and M. M. Oliveira, "On the experience of groundwater vulnerability assessment in Portugal," *Aquifer Vulnerability and Risk International Workshop AVR03, Salamanca Gto. Mexico*, 2003.
- [57] I. S. Zekster, *Groundwater and the environment*. London, New York: Lewis Publishers, 2000.